

Dominant Effect of Antiangiogenesis in Combination Therapy Involving Cyclophosphamide and Axitinib

Jie Ma and David J. Waxman

Abstract Purpose: Antiangiogenic drug treatment inhibits tumor growth by decreasing blood supply, which can also reduce the delivery of other therapeutic agents. Presently, we investigated the effect of the vascular endothelial growth factor receptor tyrosine kinase inhibitor axitinib (AG-013736) on tumor vascular patency and chemotherapeutic drug uptake. Furthermore, the effect of axitinib on the antitumor activity of combination treatments with cyclophosphamide was examined.

Experimental Design: Prostate cancer PC-3 xenografts were used to evaluate the effect of axitinib treatment on tumor vascular morphology, fluorescent dye perfusion, hypoxia, and uptake of 4-hydroxycyclophosphamide, the active metabolite of the chemotherapeutic prodrug cyclophosphamide. Sequential or simultaneous schedules for axitinib and cyclophosphamide administration were evaluated in both PC-3 tumors and 9L gliosarcoma xenograft models.

Results: Axitinib monotherapy induced sustained growth stasis in PC-3 tumors in association with extensive apoptotic cell death. A substantial decrease in tumor vascular patency was observed, exemplified by a near complete loss of Hoechst 33342 perfusion and the absence of pimonidazole staining in the increasingly hypoxic tumors. Antitumor activity was significantly enhanced in both PC-3 and 9L tumors treated using an optimized schedule of sequential, intermittent axitinib-cyclophosphamide combination therapy despite a 40% to 70% decrease in tumor tissue uptake of 4-hydroxycyclophosphamide.

Conclusions: In axitinib-cyclophosphamide combination therapy, enhanced anticancer activity can be achieved when the reduced tumor cell exposure to the cancer chemotherapeutic agent is compensated by antiangiogenesis-induced tumor cell starvation. This intrinsic antitumor effect was particularly evident in PC-3 tumor xenografts, where tumor blood flow deprivation dominates the overall therapeutic response.

Following the approval of several antiangiogenic agents (e.g., bevacizumab, sorafenib, and sunitinib) for cancer treatment, antiangiogenesis has emerged as a new treatment option for clinical oncologists. These agents offer extended survival in patients with metastatic colorectal cancer, non-small cell lung cancer, and advanced renal cell carcinoma (1). Because antiangiogenic drugs are typically cytostatic, further development of this new class of anticancer drugs will require effective integration with conventional cytoreductive regimens (2, 3). Bevacizumab, an anti-vascular endothelial growth factor (VEGF) antibody, and the VEGF receptor (VEGFR)-2-specific

antibody DC101, both inhibit angiogenesis by blocking the binding of VEGF to its cell surface receptors. Moreover, both agents induce the morphologic and functional normalization of the tumor vasculature, which is accompanied by a transient increase in the delivery of drugs and oxygen to tumor cells (4–7). This normalization involves the pruning of immature blood vessels, a closer association between pericytes and endothelial cells, and an overall improvement in blood vessel organization (8). These changes in tumor vasculature provide a window of opportunity for increasing antitumor activity by combining cytotoxic reagents with angiogenesis inhibitors. Indeed, the survival benefits of bevacizumab treatment in clinical trials were observed in combination with cancer chemotherapeutic drugs (9).

Antiangiogenic therapy is thought to require continuous or near-continuous drug exposure *in vivo*; consequently, the initial induction of tumor vascular normalization described above is typically followed by a decrease in tumor vascular patency (8). This may eventually lead to reduced tumor uptake of a coadministered chemotherapeutic drug with loss of therapeutic activity. Moreover, not all antiangiogenic drugs induce a short-term improvement in tumor blood perfusion. Many small-molecule angiogenesis inhibitors target downstream signaling pathways, including VEGFRs and other ligand-activated receptors with tyrosine kinase activity (10). These receptor tyrosine

Authors' Affiliation: Division of Cell and Molecular Biology, Department of Biology, Boston University, Boston, Massachusetts

Received 5/5/08; revised 6/27/08; accepted 8/12/08.

Grant support: NIH grant CA49248 (D.J. Waxman).

The costs of publication of this article were defrayed in part by the payment of page charges. This article must therefore be hereby marked *advertisement* in accordance with 18 U.S.C. Section 1734 solely to indicate this fact.

Note: Supplementary data for this article are available at Clinical Cancer Research Online (<http://clincancerres.aacrjournals.org/>).

Requests for reprints: David J. Waxman, Division of Cell and Molecular Biology, Department of Biology, Boston University, 5 Cummington Street, Boston, MA 02215. Fax: 617-353-7404; E-mail: djw@bu.edu.

©2009 American Association for Cancer Research.
doi:10.1158/1078-0432.CCR-08-1174

Translational Relevance

An important consideration when introducing antiangiogenesis treatments into the clinic is their effect on tumor uptake of cytotoxic drugs and, consequently, the effect on combination therapies that incorporate these new agents. The present studies use tumor xenograft models to investigate these issues for the VEGFR tyrosine kinase inhibitor and antiangiogenesis drug axitinib, which is shown to substantially decrease tumor vascular patency and tumor uptake of 4-OH-CPA, the activated metabolite of cyclophosphamide formed in the liver. Despite this decrease in cytotoxic drug uptake, the axitinib-cyclophosphamide combination shows enhanced antitumor activity when using an optimized sequence and schedule of drug administration, indicating that these important treatment variables need to be selected carefully in the clinic. Moreover, prostate cancer PC-3 tumors are shown to be highly sensitive to antiangiogenesis despite their poor vascularity, which may be an important consideration for patient selection. Finally, the inability of the widely used hypoxia-specific dye pimonidazole to stain increasingly hypoxic PC-3 tumors following axitinib treatment indicates a need to use alternative monitors to evaluate tumor oxygenation. This is particularly true when the penetration of pimonidazole itself may be inhibited by the drug treatment under investigation.

kinase inhibitors block both cell surface and intracellular VEGF signaling pathways, resulting in irreversible endothelial cell death (11). Unlike bevacizumab, monotherapy with receptor tyrosine kinase inhibitors, such as sorafenib and sunitinib, significantly increases progression-free survival in phase III clinical trials (12, 13). Suppression of angiogenesis per se could thus be an important mode of antitumor action for these potent receptor tyrosine kinase inhibitors. Moreover, increased tumor cell starvation following angiogenesis inhibition could potentially offset any decrease in antitumor activity associated with the reduced tumor uptake of coadministered cytotoxic drugs. Antiangiogenesis may also chemosensitize tumor cells to chemotherapeutics or interfere with the repair of cytotoxic drug-induced damage (14, 15). Detailed investigation of the interactions between antiangiogenic agents and conventional cytotoxic drug treatments are required to elucidate these issues and to help identify the most effective drug combinations and schedules.

Different tumors may display distinct intrinsic sensitivities to angiogenesis inhibition. Although tumor vascular density has been widely investigated as a prognostic marker, its value in predicting tumor responses to antiangiogenic drugs is still unclear. Even less is known about how tumor vascularity, particularly the low vascular density of certain tumors, may affect antitumor activity in the context of combination therapy. Answers to these questions may provide important information for patient stratification and guide the selection of treatment regimens that include antiangiogenic drugs.

The present study was designed to investigate the effect of angiogenesis inhibition on tumor blood perfusion and chemotherapeutic drug uptake following treatment with

axitinib, a potent receptor tyrosine kinase inhibitor that targets VEGFRs at subnanomolar concentrations (16) and has shown clinical efficacy in phase II clinical trials (17, 18). The efficacy of combination therapies involving axitinib and the cytotoxic prodrug cyclophosphamide using either metronomic or maximum tolerated dose (MTD) treatment schedules was also examined. Our findings show that PC-3 human prostate cancer xenografts, which are hypovascularized, are highly sensitive to axitinib treatment. Axitinib not only induces a strong antiangiogenic response but also dominates the overall antitumor activity of drug combinations with cyclophosphamide. As a consequence, despite a substantial decrease in exposure of the axitinib-treated tumors to the active 4-hydroxycyclophosphamide (4-OH-CPA) metabolite, a significant therapeutic enhancement is achieved when cyclophosphamide is included in the combination therapy. Furthermore, our findings suggest that the therapeutic outcome of the combination therapy can be influenced by the timing of different treatment regimens, which may need to be optimized in a tumor-dependent manner. Taken together, these studies support the therapeutic potential of combining axitinib with conventional chemotherapeutic drugs for treatment of prostate cancer and potentially other tumors.

Materials and Methods

Supplementary materials and methods. Details on chemicals, cell growth inhibition, immunohistochemistry, pimonidazole staining, TUNEL assay, and image analysis are provided in Supplementary Materials together with Supplementary Figs. S1 to S5.

Cell lines. Human tumor cell lines PC-3 (prostate cancer), A549 (non-small cell lung cancer), MCF-7 (breast cancer), and U251 (glioblastoma) were obtained from Dr. Dominic Scudiero (National Cancer Institute) and were grown in RPMI 1640 containing 5% fetal bovine serum at 37°C in a humidified 5% CO₂ atmosphere. The rat gliosarcoma cell line 9L and a derivative expressing the cyclophosphamide-activating cytochrome P450 2B11 (9L/2B11 cells) were those described previously (19) and were grown in DMEM with 10% fetal bovine serum.

Tumor xenograft models. The effect of drug treatment on tumor growth was studied in PC-3 and 9L/2B11 tumor xenografts grown in *scid* mice (see below). These two tumor cell lines were selected because of their distinct differences in tumor vascularity, sensitivity to axitinib treatment both *in vivo* and *in vitro*, and their responses to metronomic cyclophosphamide treatment (19–21). For example, 9L and 9L/2B11 tumors are highly vascularized, whereas PC-3 tumors are poorly vascularized (Supplementary Fig. S1A). This morphologic difference has functional consequences, with untreated PC-3 tumors containing large hypoxic regions, whereas untreated 9L (and 9L/2B11) tumors are devoid of hypoxia as indicated by pimonidazole and glucose transporter type-1 (Glut-1) staining (Supplementary Fig. S1B). Discrete, small clusters of cells are seen in the Hoechst 33342 perfusion staining pattern of PC-3 tumors, whereas a mixture of patchy staining of separate cell clusters and near-uniform staining in some extended areas characterize 9L tumors (Supplementary Fig. S1C).

Immunodeficient male Fox Chase ICR *scid* mice, 5 to 7 weeks old, were purchased from Taconic and housed in the Boston University Laboratory of Animal Care Facility in accordance with approved protocols and federal guidelines. Autoclaved cages containing food and water were changed once a week. Mouse body weight was measured every 3 to 4 days. On the day of tumor cell inoculation, PC-3 and 9L/2B11 tumor cells at 70% to 80% confluence were trypsinized and resuspended in fetal bovine serum-free culture medium. 9L/2B11 (4×10^6) or PC-3 (6×10^6) cells in a volume of 0.2 mL were injected subcutaneously into each flank of the mouse

bilaterally. Tumor sizes were measured every 3 to 4 days using digital calipers (VWR International) and volumes were calculated as $(\pi / 6) \times (L \times W)^{3/2}$. Mice were randomized to different treatment groups on the day of initial drug treatment when the average tumor volume reached 400 to 600 mm³ (10-34 tumors per group, as specified).

Drug treatment schedules. Axitinib was suspended at 5 mg/mL polyethylene glycol 400 and sonicated at room temperature for 10 to 20 min to obtain a fine suspension. The pH was adjusted to 2 to 3 using 0.1 N HCl followed by the second sonication. A final 3:7 (v/v) ratio of polyethylene glycol 400/H₂O was obtained by adding acidified water (pH 2-3). The injection-ready solution was prepared fresh every 4 to 5 days and stored at 4°C in the dark. Axitinib was administered to the tumor-bearing mice daily by intraperitoneal injection at 25 mg/kg body weight and in a volume of 5 µL/g body weight. Control mice received daily intraperitoneal injection of vehicle solution (30% polyethylene glycol 400/70% acidified water, pH 2-3) in a volume of 5 µL/g body weight.

Freshly prepared cyclophosphamide dissolved in PBS (140 mmol/L NaCl, 10 mmol/L Na₂HPO₄, 2.7 mmol/L KCl, 1.8 mmol/L KH₂PO₄) was filtered through a 0.2 µm acrodisc syringe filter (Pall Corp.) and administered by intraperitoneal injection at either 140 mg/kg body weight every 6 days (metronomic schedule; refs. 22-24) or two injections at 150 mg/kg body weight spaced 24 h apart, with the second treatment cycle repeated after a 19-day drug-free recovery period (MTD schedule).

In MTD cyclophosphamide-axitinib combination treatment studies, two daily cyclophosphamide treatments were followed by 6 or 9 days of daily axitinib administration (or daily axitinib for 6 to 9 days as indicated followed by two daily cyclophosphamide treatments, as indicated), with each drug treatment given 24 h after the prior drug treatment. In studies where cyclophosphamide (metronomic schedule) and axitinib were to be administered on the same day, cyclophosphamide was injected 4 h before axitinib to minimize the potential for drug interactions at the level of hepatic cyclophosphamide metabolism (21).

Hoechst 33342 perfusion. Hoechst 33342, a DNA-binding fluorescent dye with molecular weight of 561, has been widely used to study the patency of the tumor vasculature (25). In the present study, Hoechst 33342 was used to determine the effect of various drug treatments on tumor blood perfusion. Stock solutions of 16 mmol/L Hoechst 33342 in PBS were stored at 4°C in the dark. One minute after tail vein injection at 15 mg Hoechst 33342/kg body weight (40-50 µL/mouse with a 29-gauge needle), tissues samples were collected and processed for cryosectioning. Images were analyzed using a fluorescent microscope and captured by an Olympus MagnaFire digital camera. Representative fields of the staining patterns were presented for each tissue.

Tumor uptake of 4-OH-CPA. The effect of each drug treatment on the net uptake of 4-OH-CPA by PC-3 tumors was determined as follows. A single intraperitoneal injection of cyclophosphamide (140 mg/kg body weight) was administered to tumor-bearing mice 24 h after the last axitinib (25 mg/kg/d intraperitoneally) or cyclophosphamide treatment (140 mg/kg intraperitoneally every 6 days), except in the case of the 12 h axitinib treatment time point, where cyclophosphamide was given 12 h after axitinib. Mice were killed 15 min after cyclophosphamide injection, corresponding to the T_{max} of plasma and liver 4-OH-CPA (20, 21). Blood, liver, and tumor samples were collected and processed for analysis of 4-OH-CPA after derivatization to 7-hydroxyquinoline (26). Tissue recovery of 4-OH-CPA was 60 ± 3% with a sensitivity of 1 µmol/L under these conditions (26). Data were expressed as mean ± SE nanomoles of 4-OH-CPA produced per gram of tissue for $n = 6$ tumors (3 mice) per data point.

Statistical analysis. Results were expressed as mean ± SE and are based on the indicated number of tumors or tissue samples per group. Statistical significance of differences was assessed by two-tailed Student's *t* test or one-way ANOVA with Tukey post test as specified in the text using Prism software version 4.0 (GraphPad) with a significance level of ≤ 0.05.

Results

Axitinib treatment arrests PC-3 tumor growth by angiogenesis inhibition. Six days after the initiation of daily axitinib treatment (25 mg/kg intraperitoneally, *scid*), growth stasis was observed for PC-3 tumor xenografts grown subcutaneously in immunodeficient *scid* mice (Fig. 1A, *top*). On day 12, when the control group was terminated, the size of axitinib-treated tumors was significantly smaller than that of control tumors ($P < 0.001$, Student's *t* test). This growth stasis response was maintained for at least 24 days. Male *scid* mice bearing subcutaneous PC-3 tumors showed body weight loss beginning when the tumor volume reached 200 to 300 mm³ both with and without axitinib treatment (Fig. 1A, *bottom*), indicating no added toxicity from the axitinib treatment. Axitinib decreased PC-3 tumor vascular area by 30% (Fig. 1B, *top*) and dilated blood vessels seen in untreated PC-3 tumors became undetectable (Fig. 1B, *bottom*). However, the number of microvessels per field (already low in the untreated PC-3 tumors; Supplementary Fig. S1A) showed no significant change (Fig. 1C). In cell culture studies, micromolar concentrations of axitinib displayed growth-inhibitory activity against several tumor cell lines but not PC-3 cells (Fig. 1D), suggesting the anti-PC-3 tumor activity of axitinib *in vivo* (Fig. 1A) is not due to direct tumor cell cytotoxicity. Rather, axitinib-induced angiogenesis inhibition is likely the underlying mechanism for the observed tumor growth stasis.

Axitinib induces PC-3 tumor hypoxia and suppresses tumor blood perfusion. Untreated PC-3 tumors were hypoxic as indicated by extensive staining with the hypoxia marker Glut-1 (Fig. 2A, *left*). Glut-1 was validated as an endogenous marker for PC-3 tumor hypoxia by its substantial up-regulation in PC-3 cells cultured in hypoxic conditions (0.2% O₂ for 48 h; Supplementary Fig. S2A). Glut-1 staining colocalized with the hypoxia-specific dye pimonidazole in untreated PC-3 tumors (Supplementary Fig. S2B) and was largely exclusive of CD31 (endothelial cell) staining (Supplementary Fig. S2C). Quantification of Glut-1 staining in PC-3 tumors revealed a 27% increase in Glut-1-positive area following axitinib treatment, evidencing drug-induced tumor hypoxia (Fig. 2A, *right*). In contrast, staining with the exogenous hypoxia marker pimonidazole showed a time-dependent decrease in PC-3 tumor staining, with only small regions on the tumor periphery stained after 24 days of axitinib treatment (Fig. 2B). Given the increase in Glut-1 staining (Fig. 2A), the decrease in pimonidazole staining does not indicate a decrease in tumor hypoxia; rather, it most likely results from decreased delivery of the hypoxia-responsive dye itself to the hypoxic regions of axitinib-treated tumors.

The significant change in PC-3 tumor vascular patency indicated by these findings was verified by Hoechst 33342 perfusion, which stained individual cell clusters in untreated PC-3 tumors (Fig. 2C), indicating the presence of perfused blood vessels. After 24 days of axitinib treatment, when pimonidazole staining in PC-3 tumors was undetectable, Hoechst 33342 staining was also undetectable. Careful examination of Hoechst 33342 staining in several normal tissues, including heart, kidney, liver, lung, and muscle, revealed no significant changes in blood perfusion following axitinib treatment, although a small decrease in staining intensity was apparent in intestine (Fig. 2D). Thus, axitinib significantly and

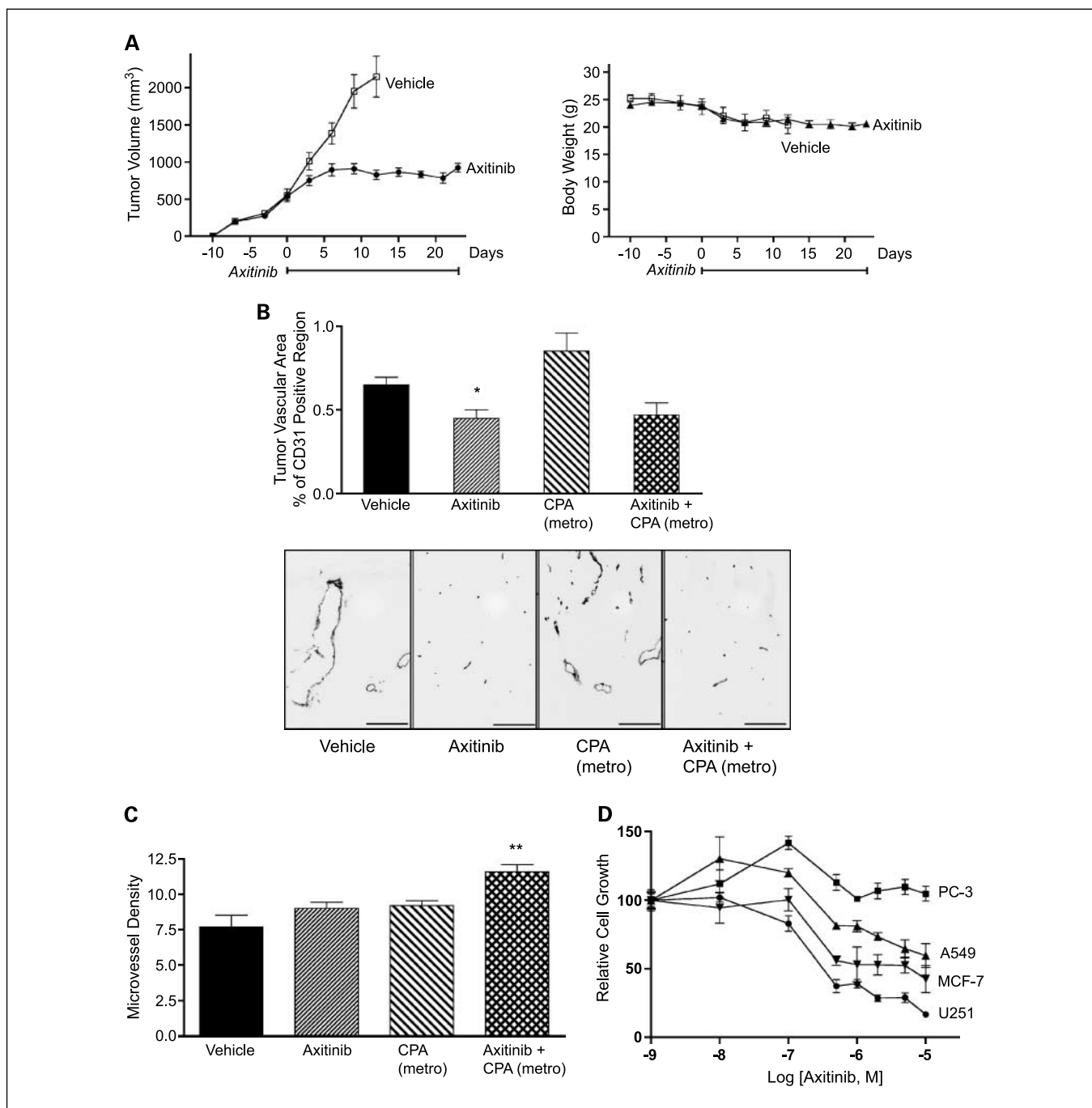


Fig. 1. Antitumor activity and antiangiogenic effects of axitinib in PC-3 tumor xenografts and cultured tumor cells. *A*, axitinib monotherapy (25 mg/kg intraperitoneally daily, days 0-23) induced growth stasis in PC-3 tumor xenografts grown subcutaneously in immunodeficient *scid* mice. Limited body weight loss was associated with tumor growth but was not increased by axitinib treatment (*right*; 4-6 g loss over a 22-day period in 5-week-old male *scid* mice beginning when the tumor volume reached 200-300 mm³). *Solid line beneath the X axis*, period of daily axitinib treatment. Data are based on *n* = 10 tumor per group. *Bars*, SE. *B*, percentage of surface area of PC-3 tumor cryosections that stained CD31 positive (*top*). Daily axitinib treatment for 24 d but not metronomic cyclophosphamide treatment (140 mg/kg intraperitoneally every 6 d × 4 cycles) significantly reduced tumor vascular area (mean ± SE, *n* = 4 tumors per group). Dilated blood vessels were not detected in axitinib-treated or combination therapy-treated PC-3 tumors (*bottom*). Bar, 200 μm. *C*, number of tumor blood vessels per CD31-immunostained PC-3 tumor section counted at ×400 magnification. The decrease in vascular area (*B*) without a change in microvessel density (*C*) following axitinib monotherapy suggests that the remaining blood vessels are smaller in size. Mean ± SE (*n* = 4 tumors per group). *, *P* < 0.05; **, *P* < 0.01, compared with vehicle control (Student's *t* test). *D*, cultured PC-3, A549, MCF-7, and U251 tumor cells were continuously treated with axitinib at the indicated concentrations for 4 d and the effect on final cell numbers, indicative of relative growth rate, was determined by crystal violet staining. Mean ± SD (*n* = 3 replicates per data point).

specifically reduces PC-3 tumor vascular patency without affecting most normal tissues.

Axitinib rapidly but reversibly decreases tumor uptake of 4-OH-CPA. Given the near-complete block in the delivery of both

Hoechst 33342 and pimonidazole into axitinib-treated PC-3 tumors, we investigated the effect of axitinib treatment on PC-3 tumor uptake of 4-OH-CPA, the cytotoxic metabolite of cyclophosphamide formed in the liver via cytochrome *P450*

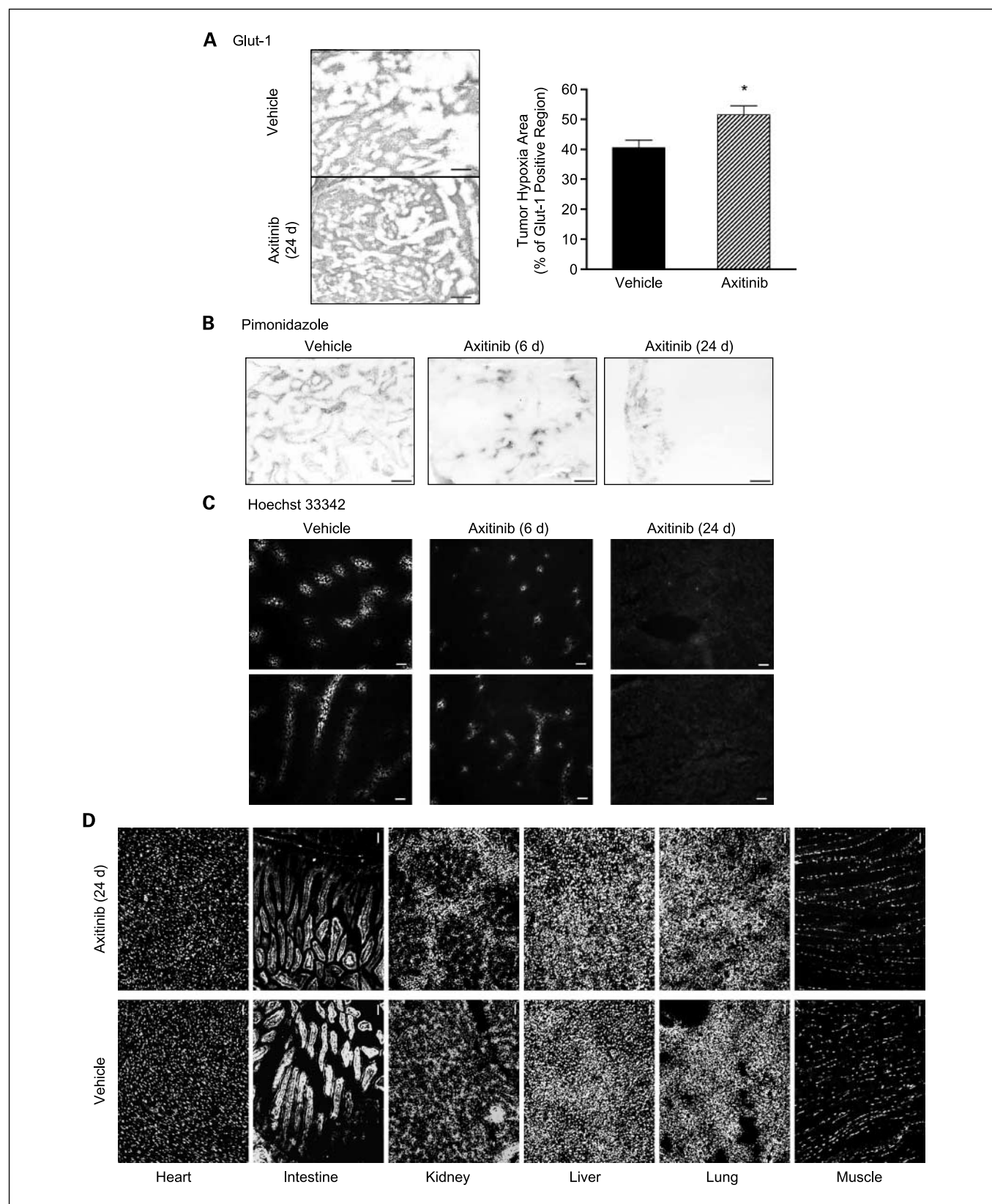


Fig. 2. Axitinib treatment reduces PC-3 tumor vascular patency without affecting normal tissues. *A*, immunostaining of the endogenous hypoxia marker Glut-1 revealed extensive hypoxia in PC-3 tumors (*left*). Quantification of Glut-1-positive area revealed increased tumor hypoxia following daily axitinib treatment (25 mg/kg intraperitoneally daily) for 24 d (*right*). Mean \pm SE ($n = 4$ tumors per group). *B*, staining with the hypoxia-specific dye pimonidazole in untreated PC-3 tumors gradually decreases following 6 and 24 d of axitinib treatment. Bar, 500 μ m (*A* and *B*). Vascular patency of PC-3 tumors (*C*) and normal tissues (*D*) was determined by intravenous injection of Hoechst 33342 dye (15 mg/kg) followed by 1 min of circulation. Bar, 50 μ m (*C* and *D*).

metabolism. Although axitinib does not inhibit the activation of cyclophosphamide by liver cytochrome P450 enzymes or the export of 4-OH-CPA from liver to blood (21), PC-3 tumor uptake of 4-OH-CPA decreased to 60% of control 12 h after a single axitinib injection followed by a further decrease to 30% of control after 24 days of axitinib treatment (Fig. 3A). This 70% decrease in tumor drug uptake is more extensive than the 30% decrease in tumor vascular area (Fig. 1B), suggesting that axitinib both prunes tumor blood vessels and decreases the patency of the remaining vessels.

Next, we investigated whether the inhibition of tumor drug uptake by axitinib is reversible. PC-3 tumors were treated with axitinib for 6 days, at which time drug treatment was discontinued and the capacity for tumor uptake of 4-OH-CPA was determined. Although the half-life of axitinib in mouse plasma is only 2 h (16), PC-3 tumor 4-OH-CPA levels did not fully recover until 6 days after axitinib withdrawal (Fig. 3B, fourth column). This reversal of the antivasular effects of axitinib was accompanied by a resumption of tumor growth (Fig. 3C). A second cycle of axitinib was administered 9 days after the termination of the first axitinib treatment cycle, which inhibited tumor uptake of 4-OH-CPA within 12 h (Fig. 3B, last column versus sixth column), similar to the initial axitinib treatment (Fig. 3A, day 0.5). Thus, the tumor blood vessels remain sensitive to axitinib inhibition.

Axitinib reduces tumor cell proliferation and increases apoptosis. Next, we investigated the inhibitory effect of axitinib on PC-3 tumor cell proliferation. PC-3 tumor expression of proliferation cell nuclear antigen was measured by immunohistochemical staining, which showed a >50% decrease in proliferation index after 24 days of axitinib treatment (Fig. 4A). At the same time, the level of apoptosis (TUNEL staining) was increased in axitinib-treated PC-3 tumors (Fig. 4B). Large areas of PC-3 tumors showed condensed nuclear staining following axitinib treatment (Supplementary Fig. S3), suggesting that there is extensive apoptosis or necrosis in the axitinib-treated tumors. Because axitinib does not directly inhibit PC-3 tumor cell growth (Fig. 1D), this antiproliferation activity, and the associated proapoptotic response, is likely to be secondary to the axitinib-induced decrease in tumor blood perfusion and the increase in hypoxia (Figs. 2 and 3). Thus, strong angiogenesis inhibition induces substantial tumor cell starvation and death, which itself has an important inhibitory effect on PC-3 tumor growth.

Improved antitumor activity of axitinib-cyclophosphamide combination. Next, we investigated the effect of the reduced tumor 4-OH-CPA uptake on the antitumor activity of axitinib-cyclophosphamide combination therapies. Two schedules of cyclophosphamide treatment were investigated: metronomic (every 6 days) cyclophosphamide, which has intrinsic antiangiogenic activity (22), and classic MTD cyclophosphamide treatment. Metronomic cyclophosphamide arrested PC-3 tumor growth after the second cycle of drug treatment (Fig. 5A). This delayed antitumor response was similar to the response to axitinib treatment. In contrast, metronomic cyclophosphamide combined with axitinib halted tumor growth on initiation of drug treatment and was followed by sustained growth stasis with a slow but steady 20% decline in tumor size, which was significantly different from the axitinib and the metronomic cyclophosphamide monotherapy groups ($P < 0.001$, one-way ANOVA, days 0-23). When drug treatment was terminated on

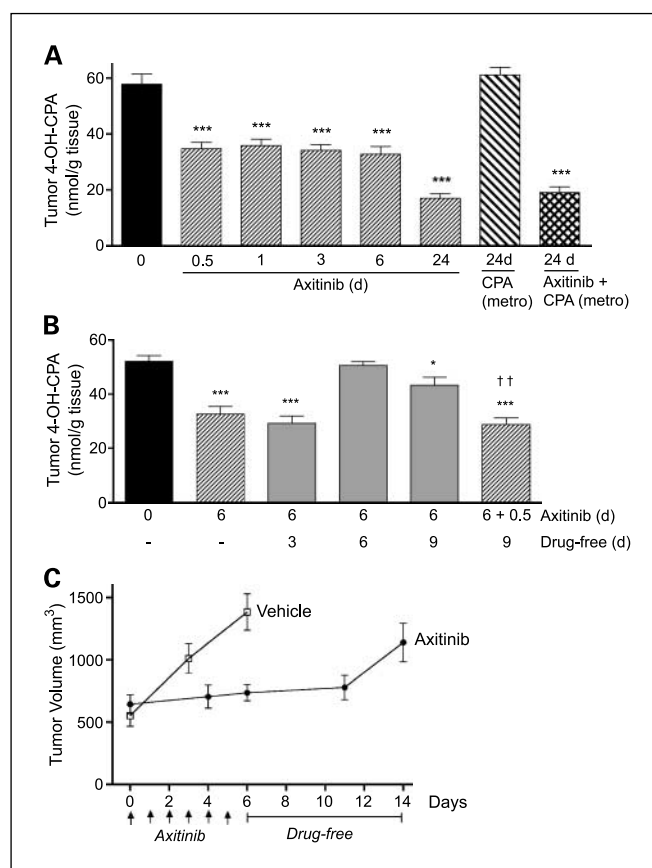


Fig. 3. Effect of axitinib on PC-3 tumor 4-OH-CPA exposure. 4-OH-CPA concentrations were determined in PC-3 tumors grown subcutaneously in *scid* mice treated with axitinib (25 mg/kg intraperitoneally daily) and/or metronomic cyclophosphamide (140 mg/kg intraperitoneally every 6 d) for the indicated periods. To determine the effect of drug treatment on tumor uptake of 4-OH-CPA, mice were given an intraperitoneal injection of a test dose of cyclophosphamide (140 mg/kg) and tumors were excised 15 min later. Tumor levels of 4-OH-CPA were determined by high-performance liquid chromatography. **A**, intratumoral 4-OH-CPA levels were decreased to 60% of control within 12 h (0.5 day) after the first axitinib injection and to 30% of control after 24 d of axitinib treatment both without and with metronomic cyclophosphamide treatment (*metro*). **B**, daily injection of axitinib for 6 d reduced tumor 4-OH-CPA uptake by ~40% (*second column* compared with *first column*). This decrease was largely reversed 6 d after the cessation of drug treatment (*fourth column* compared with *first column*). Tumor 4-OH-CPA uptake decreased again within 12 h after a second cycle of axitinib treatment (*last column* compared with *fifth column*). *, $P < 0.05$; ***, $P < 0.001$, compared with day 0 control (*first column*); ††, $P < 0.01$, compared with axitinib day 6/drug-free day 9 (*fifth column*), Student's *t* test ($n = 6$ tumors per group). **Bars**, SE (A) and (B). **C**, PC-3 tumors undergoing growth stasis following axitinib treatment (25 mg/kg intraperitoneally d 0-5) resumed growth 6 d after drug withdrawal. *Arrows beneath the X axis*, days of axitinib treatment. Data represent $n = 6$ tumors per group. **Bars**, SE.

day 23, PC-3 tumors given the combination treatment were significantly smaller than tumors treated with either monotherapy alone (Student's *t* test, $P < 0.001$). The reduced vascular area and small increase in microvessel density seen in the combination treatment group (Fig. 1B, top, and 1C) largely reflect changes associated with axitinib treatment. In addition, axitinib decreased intratumoral 4-OH-CPA (Fig. 3A, last three columns) and markedly increased apoptosis (Fig. 4B) both with and without metronomic cyclophosphamide treatment. Thus, axitinib plays a dominant role in the antitumor activity of the combination therapy.

MTD cyclophosphamide treatment induced substantial PC-3 tumor growth delay at the first treatment cycle followed by a shorter delay after the second cycle of drug treatment (Fig. 5B). Neoadjuvant axitinib treatment for 9 days followed by MTD cyclophosphamide resulted in sustained PC-3 tumor growth stasis through two cycles of drug treatment (Fig. 5B) despite the 40% to 70% decrease in tumor uptake of 4-OH-CPA (Fig. 3A). However, the strongest anti-PC-3 tumor growth response was achieved with another drug administration schedule, where MTD cyclophosphamide was followed by 9 days of axitinib treatment. With this schedule, not only was tumor growth

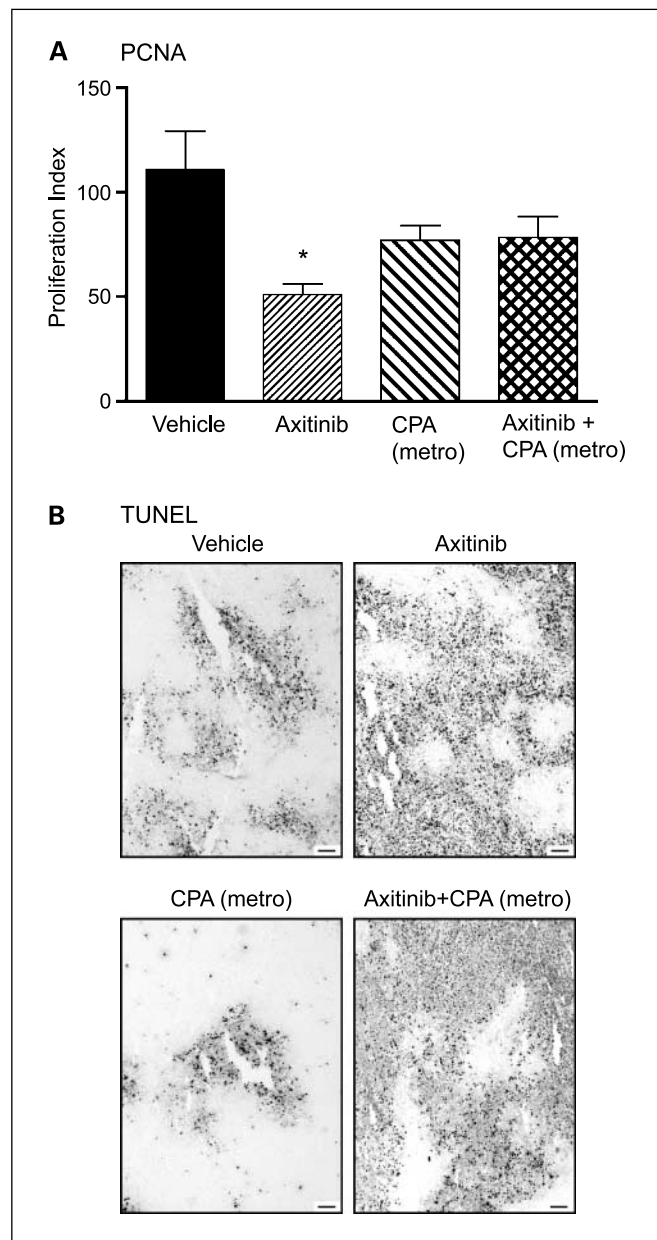


Fig. 4. Cell proliferation and apoptosis in 24-d axitinib and/or 4 x 6 d metronomic cyclophosphamide-treated PC-3 tumors. Effect of the indicated *in vivo* drug treatments on PC-3 tumor cell proliferation (A) and apoptosis (B) was analyzed by proliferation cell nuclear antigen immunostaining and TUNEL assay, respectively. The number of proliferation cell nuclear antigen-positive cells were counted at x200 magnification. *, $P < 0.05$, compared with vehicle control for $n = 4$ tumors per group (Student's *t* test). Bar, 100 μ m.

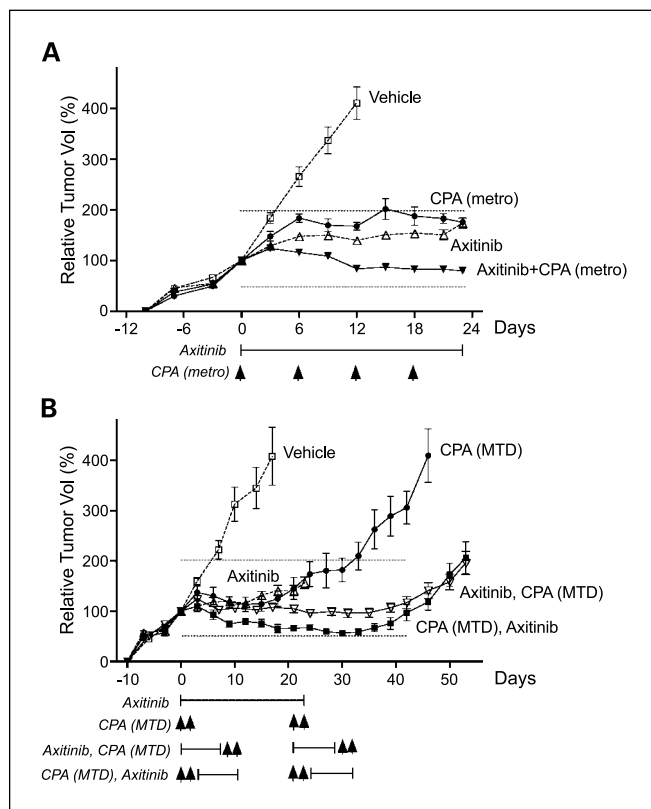


Fig. 5. Antitumor activity of cyclophosphamide-axitinib combination therapy in PC-3 tumors. PC-3 tumors were implanted subcutaneously in *scid* mice. Arrows along the X axis, days on which cyclophosphamide was administered; horizontal lines below the X axis, period of daily axitinib treatment (25 mg/kg intraperitoneally, daily). Tumor volumes are expressed as a percentage of the volume on day 0, when drug treatment was initiated, to facilitate comparisons between groups. Dotted horizontal lines above the X axis, a 50% decrease (bottom line) and a 100% increase in tumor volume (top line), respectively. A, combination of daily axitinib treatment with metronomic cyclophosphamide (140 mg/kg intraperitoneally every 6 d) led to tumor growth arrest by the second cyclophosphamide injection. B, antitumor activity of MTD cyclophosphamide (150 mg/kg, two intraperitoneal injections 24 h apart, repeated every 21 d) was significantly enhanced when followed by 9 d of daily axitinib treatment. $P < 0.01$, one-way ANOVA, days 0 to 42. No body weight loss was induced by the various combination drug treatments compared with vehicle-treated tumor-bearing mice (see Supplementary Fig. S4). Data represent $n = 10$ to 24 tumors per group. Bars, SE.

completely arrested on initiation of drug treatment, but also the tumors gradually regressed, with a maximal regression of close to 50% achieved during the second cycle of combination therapy (Fig. 5B). A near-identical antitumor response was seen when daily axitinib treatment was extended for 19 days, until the next cycle of MTD cyclophosphamide treatment (data not shown), where the absence of an axitinib-free interval between cyclophosphamide treatments excludes the possibility that tumor 4-OH-CPA uptake recovers by the time of the second cycle of cyclophosphamide treatment (Fig. 3B). Tumor volumes of both combination treatment groups (axitinib/MTD cyclophosphamide and MTD cyclophosphamide/axitinib) were significantly different from the MTD cyclophosphamide treatment group ($P < 0.001$, one-way ANOVA, days 0-56) and from each other ($P < 0.01$, one-way ANOVA, days 0-42). Quantification of the MTD cyclophosphamide-induced tumor growth delay periods revealed the following tumor volume doubling times: 4 days (vehicle control), 32 days (MTD cyclophosphamide), 53 days (axitinib/MTD cyclophosphamide), and 53 days

(MTD cyclophosphamide/axitinib). Tumors treated with axitinib monotherapy were significantly larger than those in either combination treatment group ($P < 0.001$, Student's t test, day 23). PC-3 tumor-induced body weight loss was similar in all treatment groups (Supplementary Fig. S4), indicating that the combination of cyclophosphamide with axitinib does not cause additional host toxicity.

Optimal timing of axitinib and cyclophosphamide administration in 9L/2B11 tumor model. *scid* mice bearing 9L gliosarcoma expressing the cyclophosphamide-activating cytochrome P450 2B11 (9L/2B11 tumors) were used as a second model to investigate the therapeutic effect of combining axitinib with MTD cyclophosphamide. In 9L/2B11 tumors, overall antitumor activity was increased when MTD cyclophosphamide was followed by daily axitinib treatment (Fig. 6), a finding that is consistent with, but less dramatic than, our results with PC-3 tumors (Fig. 5B). In contrast to PC-3 tumors, however, an even greater increase in anti-9L/2B11 tumor activity was seen when neoadjuvant axitinib treatment preceded MTD cyclophosphamide treatment (Fig. 6). This improvement was obtained despite the limited antitumor activity of axitinib alone in 9L/2B11 tumors (Fig. 6) and despite the decrease in tumor uptake of 4-OH-CPA (21). One-way ANOVA analysis of tumor volume changes in the last cycle of drug treatment (days 48-69) verified that all three treatment groups were significantly different from each other ($P < 0.01$). Thus, axitinib/MTD cyclophosphamide was more effective than MTD cyclophosphamide/axitinib, which itself was more effective than MTD cyclophosphamide alone. A small body weight loss occurred after each cyclophosphamide treatment cycle (Supplementary Fig. S5), as is typical for MTD-scheduled cytotoxic drugs.

Discussion

As new antiangiogenesis drugs enter the clinic for cancer treatment and an even larger number of candidates progress

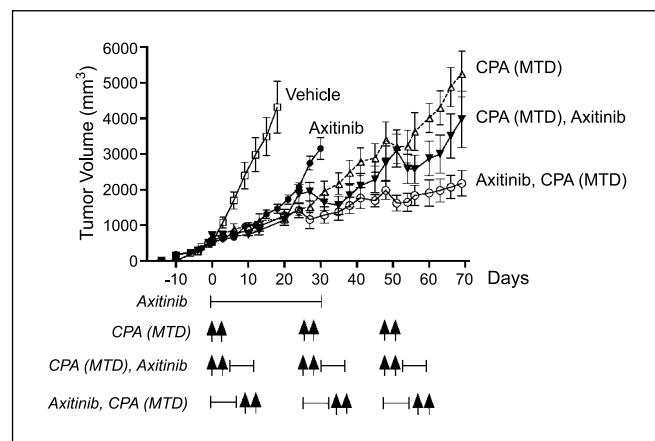


Fig. 6. Effect of relative timing of axitinib versus cyclophosphamide administration on 9L/2B11 antitumor activity. 9L/2B11 rat gliosarcoma tumors implanted subcutaneously in 5-week-old *scid* mice were treated with axitinib and/or MTD cyclophosphamide using doses as specified in Fig. 5 and the following schedules as summarized in the diagrams below the X axis: daily axitinib for 30 d; MTD cyclophosphamide, 3 cycles repeated every 24 d; MTD cyclophosphamide either preceding or following 6 daily treatments with axitinib. Drug treatment was initiated when the average tumor volume reached $\sim 500 \text{ mm}^3$ (day 0). Six days of neoadjuvant axitinib treatment showed the strongest antitumor activity without any drug-associated body weight loss (see Supplementary Fig. S5). Mean \pm SE ($n = 10$ tumors per group).

through preclinical and clinical development, it is important to obtain a better understanding of their effects on tumor blood vessel patency and their potential interactions with traditional cancer chemotherapies. In the current study, we investigated axitinib, an oral antiangiogenic drug and potent and selective inhibitor of VEGFR-1, VEGFR-2, and VEGFR-3, which has shown substantial antitumor activity in multiple preclinical models and in several clinical trials (17, 21, 28). Specifically, we investigated how axitinib affects tumor blood perfusion in human prostate cancer PC-3 xenografts and the potential effect of such changes have on the efficacy of axitinib in combination with the cancer chemotherapeutic prodrug cyclophosphamide. PC-3 tumor blood vessel patency was significantly reduced by axitinib, which substantially blocked tumor cell access to pimonidazole, Hoechst 33342, and 4-OH-CPA, the active, cytotoxic metabolite of cyclophosphamide, all delivered via tumor blood flow. Despite the unfavorable effect on tumor uptake of 4-OH-CPA, the antitumor activity of axitinib in combination with cyclophosphamide was found to be greater than that of either agent alone. The present study also suggests that the intrinsic vascularity of a given tumor may influence its responsiveness to angiogenesis inhibition, as PC-3 tumors, which are poorly vascularized, showed substantially greater sensitivity to axitinib treatment (Fig. 1A) than 9L gliosarcoma, which are highly vascularized (21). Finally, studies with PC-3 tumors and with 9L tumors expressing the cyclophosphamide-activating cytochrome P450 2B11 (19, 20) revealed that the relative timing of axitinib and cyclophosphamide administration can significantly affect the antitumor activity of the combination. Thus, optimization of combination therapies will require careful consideration of the effect of intrinsic tumor vascularity and the diverse interactions that may occur between angiogenesis inhibitors and cytotoxic chemotherapeutic agents.

Multiple methods have been developed for measuring tissue oxygenation, including polarographic needle electrodes, fluorescent fiber probes (29), electron paramagnetic resonance oximetry (30), and hypoxia-specific dyes (31). Pimonidazole, a 2-nitroimidazole derivative (Hypoxprobe), is enzymatically reduced at low oxygen tensions and forms protein adducts, which can be visualized using specific antibody (32). Pimonidazole is widely used for detection of hypoxia *in vivo*, including tumor hypoxia induced by antiangiogenic drugs (4, 25). However, the present findings show that the reliability of pimonidazole as an indicator of tumor hypoxia can be compromised by drug-dependent reduction in tumor blood perfusion, which affects the tissue penetration of pimonidazole itself. For example, untreated PC-3 tumors showed extensive hypoxia staining following intraperitoneal delivery of pimonidazole, which is consistent with direct measurements of oxygen tension in PC-3 tumors using polarographic electrodes (33). Interestingly, this staining became undetectable after chronic axitinib treatment. Although certain antiangiogenic drugs can increase tumor oxygenation by inhibiting tumor cell mitochondrial respiration (34), this effect has not been reported for axitinib. Moreover, our monitoring of PC-3 tumor hypoxia with the endogenous hypoxia marker Glut-1, whose expression colocalized with pimonidazole staining in untreated PC-3 tumors and some other tumor types (35), revealed an increase in tumor hypoxia following axitinib treatment. Perfusion with the fluorescent dye Hoechst 33342 revealed strong staining of discrete cell clusters surrounding patent blood vessels in

untreated PC-3 tumors that was abolished by axitinib treatment. In addition, the PC-3 tumor content of liver-activated, blood-delivered 4-OH-CPA was reduced >70% by long-term axitinib treatment. Thus, the decrease in pimonidazole staining seen in axitinib-treated PC-3 tumors is not due to a decrease in tumor hypoxia per se but rather results from the inability of the dye to efficiently penetrate into the tumor via blood circulation. Therefore, when strong inhibition of tissue blood perfusion may occur, exogenous hypoxia-sensitive dyes such as pimonidazole cannot be reliably used and alternative methods, such as staining with Glut-1 or other endogenous hypoxia markers, or direct pO₂ measurements should be employed.

Surviving blood vessels in PC-3 tumors are reduced in size following axitinib or axitinib-cyclophosphamide combination treatment, suggesting there is a more pronounced effect of axitinib on larger blood vessels. Similar decreases in tumor blood vessel size have been observed with other antiangiogenesis drugs (5, 36). The antiangiogenic effects of axitinib seen in PC-3 tumors were not manifested as a decrease in blood vessel counts despite the pruning of dilated blood vessels and the significant drop in tumor blood perfusion revealed by three separate functional assays: an increase in tumor hypoxia, a decrease in Hoechst 33342 staining, and a decrease in 4-OH-CPA uptake. These observations support the conclusion that changes in tumor microvessel density should be considered carefully when assessing the antiangiogenic response of drug treatment (37). Moreover, although highly vascularized tumors are often studied as therapeutic targets for antiangiogenic drugs (38, 39), the importance of tumor vascularity as a predictor of the therapeutic efficacy of antiangiogenesis treatments is still unclear (40). In the present study, complete growth stasis was observed when axitinib was used to treat PC-3 tumors, which are hypovascularized, whereas only a transient tumor growth delay was seen in axitinib-treated 9L tumors, which are hypervascularized, despite the large decrease in 9L tumor microvessel density and the increase in 9L tumor hypoxia that accompanies drug treatment (21). Several factors may contribute to the differential responses of 9L and PC-3 tumors to antiangiogenic drug treatment, including tissue of origin, oncogenic background, and vascularity. In particular, the low vascularity of PC-3 tumors may increase tumor susceptibility to antiangiogenic drugs, such as axitinib, which may suppress tumor blood flow to a level where tumor growth cannot be supported. In contrast, the high vascular density of 9L tumors may provide a reservoir of excess blood flow capacity, which makes complete arrest of tumor growth by angiogenesis inhibition alone more difficult to achieve. Differential responses to antiangiogenic treatments have been described in a limited number of other hypervascularized versus hypovascularized tumor models (41–43). Further investigation of the effect of intrinsic tumor vascularity on the response to angiogenesis inhibition will be of great importance to the identification of suitable patient populations and the selection of treatment schedules for this new class of anticancer drugs.

Certain antiangiogenesis treatments may normalize tumor vasculature and thereby facilitate the delivery of cytotoxic drugs and oxygen to the tumor for a limited period (8) and thereby sensitize tumors to chemotherapeutic agents and radiation therapy (4, 6, 44). In combination therapies where antiangiogenic drugs alone have limited efficacy, cytotoxic chemotherapeutics are likely to dominate the antitumor response.

Consequently, any decrease in tumor blood flow induced by an antiangiogenic agent may compromise the efficacy of the combination therapy. For example, in the case of 9L tumors treated with metronomic cyclophosphamide, which as a monotherapy induces substantial tumor regression, combination with axitinib decreases tumor uptake of 4-OH-CPA and blocks cyclophosphamide-induced expression of endogenous angiogenesis inhibitor thrombospondin-1 in host cells, thereby interfering with metronomic cyclophosphamide-induced 9L tumor regression (21). Similar decreases in drug or nonspecific IgG uptake have been observed in other axitinib-treated tumors, despite the morphologic normalization of the tumor vasculature, which is indicated by decreased tortuosity, a closer association between endothelial cells and pericytes, and reduced vessel leakiness (28, 45).

In the present study of PC-3 tumors, however, despite an even greater decrease in tumor uptake of 4-OH-CPA following axitinib treatment, and the blocking of metronomic cyclophosphamide-induced host cell thrombospondin-1 expression in combination therapy-treated PC-3 tumors (data not shown), a significantly improved antitumor response was achieved with the axitinib-cyclophosphamide combination. Thus, the strong antiangiogenic action of axitinib on PC-3 tumors, which was manifested as a substantial decrease in blood flow to a tumor that is already hypovascularized, dominates the overall antitumor activity of the combination therapy. Consistent with the strong intrinsic anti-PC-3 tumor activity of axitinib, PC-3 tumors displayed several responses to the axitinib monotherapy and the combination drug treatment not seen in the cyclophosphamide alone treatment group. For example, metronomic cyclophosphamide decreased the number of TUNEL-positive cells and increased the occurrence of enlarged cell nuclei in PC-3 tumors, whereas both axitinib monotherapy and the combination treatment substantially increased apoptosis and induced a population of cells with condensed nuclei. Thus, despite the negative effect of axitinib treatment on tumor drug uptake, the cytotoxicity conferred by the residual intratumoral 4-OH-CPA supplements the antitumor activity of axitinib, which collectively enhance overall therapeutic response. Similarly, when axitinib was added to fractionated radiation therapy, despite an increase in tumor hypoxia, which would be expected to decrease tumor cell radiosensitivity, the overall antitumor effect was increased (46). Together, these observations suggest that for axitinib, and perhaps other receptor tyrosine kinase inhibitors as well, inhibition of tumor blood perfusion can itself elicit a substantial antitumor response. In such a case, the overall antitumor activity of the combination therapy will reflect the effect of angiogenesis inhibition and the response to tumor cell exposure to cytotoxic agents. Suboptimal delivery of the cytotoxic drug may be more than compensated by antiangiogenesis-induced tumor cell starvation, so that overall antitumor activity is still enhanced, despite the decrease in tumor cell exposure to the cytotoxic drug. This antitumor mechanism is likely to be most important in combination therapies using potent antiangiogenic agents, such as axitinib, and in tumors where a low level of tumor vascular patency can readily be achieved. By contrast, in tumors where the cytotoxic drug dominates the antitumor response, addition of an antiangiogenic agent may decrease the overall antitumor effect as exemplified by our earlier study with 9L tumors given axitinib in combination with metronomic

cyclophosphamide (21). Moreover, the present studies suggest that therapeutic responses may need to be optimized in a tumor type-related manner by appropriate adjustment of the schedules of antiangiogenic and chemotherapeutic drug treatment.

Cytotoxic drugs induce severe damage to both tumor cells and tumor-associated endothelial cells (22, 24). The repair processes initiated during the drug-free recovery period that follows a cycle of chemotherapy could become another target for antiangiogenic treatment in a combination therapy setting (2). Presently, the addition of axitinib as an adjuvant following MTD cyclophosphamide treatment improved the overall antitumor response, as could be anticipated. Surprisingly, however, substantial improvement in the antitumor response to MTD cyclophosphamide was also seen when a short course of axitinib therapy preceded MTD cyclophosphamide treatment, particularly for 9L/2B11 tumors. The superior 9L/2B11 antitumor activity of this neoadjuvant axitinib treatment cannot be explained by a change in the intrinsic chemosensitivity of 9L tumor cells to 4-OH-CPA (21) or by functional normalization of the tumor vasculature, because axitinib actually decreases tumor uptake of 4-OH-CPA. Timing-dependent antitumor effects are also seen when the antiangiogenic drug SU11657 is combined with radiation therapy (47), suggesting that there are intrinsic, beneficial interactions between the two therapeutic agents under this neoadjuvant schedule. These interactions not only counterbalance the negative effect of the decrease in tumor oxygenation and the reduced exposure to 4-OH-CPA but also further amplify the intrinsic antitumor activity of antiangiogenesis and/or cytoreductive regimens. Given that VEGFR-positive endothelial cells are the primary target of axitinib action, axitinib pretreatment could increase the chemosensitivity of tumor-associated endothelial cells in a manner that increases both vascular damage and tumor cell damage following cytotoxic drug treatment.

Another possible explanation involves bone marrow-derived endothelial cell progenitors, whose mobilization is induced by MTD cyclophosphamide treatment (48) but is blocked by antiangiogenic treatments including axitinib (14, 15). It has yet to be determined if axitinib, when used as an adjuvant, retains its effect on endothelial cell progenitor mobilization.

In conclusion, the VEGFR tyrosine kinase inhibitor axitinib induced a significant but reversible decrease in PC-3 tumor blood perfusion, which was sufficient to arrest tumor growth. This potent antiangiogenic effect appears to serve as the major antitumor factor in combination therapies applied to PC-3 tumors, where coadministration of cyclophosphamide further enhanced the overall antitumor response despite a substantial decrease in tumor uptake of the active chemotherapeutic agent. The relative timing of antiangiogenesis treatment and cytotoxic drug administration was also shown to affect therapeutic activity and is an important consideration for the development of combination therapies. Finally, the low intrinsic vascularity of PC-3 tumors may be an important factor in the response to angiogenesis inhibition, insofar as a further decrease in blood supply may render tumor growth unsustainable. Further understanding of the relationship between tumor vascularity and the clinical efficacy of antiangiogenic drugs may provide important guidance in patient stratification and regimen selection in cancer treatment.

Disclosure of Potential Conflicts of Interest

No potential conflicts of interest were disclosed.

Acknowledgments

We thank Pfizer Global Research and Development for providing axitinib, Drs. Dana Hu-Lowe, I. Chen, and Alison Russell (Pfizer Global Research and Development) for helpful discussions, and Chong-Sheng Chen for high-performance liquid chromatography analysis.

References

- Folkman J. Angiogenesis: an organizing principle for drug discovery? *Nat Rev* 2007;6:273–86.
- Kerbel RS. Antiangiogenic therapy: a universal chemosensitization strategy for cancer? *Science* 2006;312:1171–5.
- Gasparini G, Longo R, Fanelli M, Teicher BA. Combination of antiangiogenic therapy with other anticancer therapies: results, challenges, and open questions. *J Clin Oncol* 2005;23:1295–311.
- Winkler F, Kozin SV, Tong RT, et al. Kinetics of vascular normalization by VEGFR2 blockade governs brain tumor response to radiation: role of oxygenation, angiotensin-1, and matrix metalloproteinases. *Cancer Cell* 2004;6:553–63.
- Tong RT, Boucher Y, Kozin SV, Winkler F, Hicklin DJ, Jain RK. Vascular normalization by vascular endothelial growth factor receptor 2 blockade induces a pressure gradient across the vasculature and improves drug penetration in tumors. *Cancer Res* 2004;64:3731–6.
- Wildiers H, Guetens G, De Boeck G, et al. Effect of anti-vascular endothelial growth factor treatment on the intratumoral uptake of CPT-11. *Br J Cancer* 2003;88:1979–86.
- Dickson PV, Hamner JB, Sims TL, et al. Bevacizumab-induced transient remodeling of the vasculature in neuroblastoma xenografts results in improved delivery and efficacy of systemically administered chemotherapy. *Clin Cancer Res* 2007;13:3942–50.
- Jain RK. Normalization of tumor vasculature: an emerging concept in antiangiogenic therapy. *Science* 2005;307:58–62.
- Jain RK, Duda DG, Clark JW, Loeffler JS. Lessons from phase III clinical trials on anti-VEGF therapy for cancer. *Nat Clin Pract Oncol* 2006;3:24–40.
- Manley PW, Bold G, Bruggen J, et al. Advances in the structural biology, design and clinical development of VEGF-R kinase inhibitors for the treatment of angiogenesis. *Biochim Biophys Acta* 2004;1697:17–27.
- Lee S, Chen TT, Barber CL, et al. Autocrine VEGF signaling is required for vascular homeostasis. *Cell* 2007;130:691–703.
- Motzer RJ, Hutson TE, Tomczak P, et al. Sunitinib versus interferon α in metastatic renal-cell carcinoma. *N Engl J Med* 2007;356:115–24.
- Escudier B, Eisen T, Stadler WM, et al. Sorafenib in advanced clear-cell renal-cell carcinoma. *N Engl J Med* 2007;356:125–34.
- Paul S, Foutz T, Calleri A, et al. AG-013736, a potent VEGF/PDGF receptor tyrosine kinase inhibitor, is active against lymphoma growth and chemotherapy-induced vasculogenesis. *Blood* 2003;102:649a.
- Shaked Y, Ciarrocchi A, Franco M, et al. Therapy-induced acute recruitment of circulating endothelial progenitor cells to tumors. *Science* 2006;313:1785–7.
- Wickman G, Hallin M, Dillon R, et al. Further characterization of the potent VEGF/PDGF receptor tyrosine kinase inhibitor, AG-013736, in preclinical tumor models for its antiangiogenesis and antitumor activity. In: AACR 94th Annual Meeting; 2003 Jul 11-14; Washington, DC. p. A3780.
- George DJ. Phase 2 studies of sunitinib and AG013736 in patients with cytokine-refractory renal cell carcinoma. *Clin Cancer Res* 2007;13:753–7s.
- Rixe O, Bukowski RM, Michaelson MD, et al. Axitinib treatment in patients with cytokine-refractory metastatic renal-cell cancer: a phase II study. *Lancet Oncol* 2007;8:975–84.
- Jounaidi Y, Chen C-S, Veal GJ, Waxman DJ. Enhanced antitumor activity of P450 prodrug-based gene therapy using the low K_m cyclophosphamide 4-hydroxylase P450 2B11. *Mol Cancer Ther* 2006;5:541–55.
- Chen CS, Jounaidi Y, Su T, Waxman DJ. Enhancement of intratumoral cyclophosphamide pharmacokinetics and antitumor activity in a P450 2B11-based cancer gene therapy model. *Cancer Gene Ther* 2007;14:935–44.
- Ma J, Waxman DJ. Modulation of the antitumor activity of metronomic cyclophosphamide by the angiogenesis inhibitor axitinib. *Mol Cancer Ther* 2008;7:79–89.
- Browder T, Butterfield CE, Kraling BM, et al. Antiangiogenic scheduling of chemotherapy improves efficacy against experimental drug-resistant cancer. *Cancer Res* 2000;60:1878–86.
- Jounaidi Y, Waxman DJ. Frequent, moderate-dose cyclophosphamide administration improves the efficacy of cytochrome P-450/cytochrome P-450 reductase-based cancer gene therapy. *Cancer Res* 2001;61:4437–44.
- Ma J, Waxman DJ. Collaboration between hepatic and intratumoral prodrug activation in a P450

- prodrug-activation gene therapy model for cancer treatment. *Mol Cancer Ther* 2007;6:2879–90.
25. Franco M, Man S, Chen L, et al. Targeted anti-vascular endothelial growth factor receptor-2 therapy leads to short-term and long-term impairment of vascular function and increase in tumor hypoxia. *Cancer Res* 2006;66:3639–48.
26. Yu LJ, Drewes P, Gustafsson K, Brain EGC, Hecht JED, Waxman DJ. *In vivo* modulation of alternative pathways of P450-catalyzed cyclophosphamide metabolism: impact on pharmacokinetics and antitumor activity. *J Pharmacol Exp Ther* 1999;288:928–37.
27. Kamba T, Tam BY, Hashizume H, et al. VEGF-dependent plasticity of fenestrated capillaries in the normal adult microvasculature. *Am J Physiol Heart Circ Physiol* 2006;290:H560–76.
28. Inai T, Mancuso M, Hashizume H, et al. Inhibition of vascular endothelial growth factor (VEGF) signaling in cancer causes loss of endothelial fenestrations, regression of tumor vessels, and appearance of basement membrane ghosts. *Am J Pathol* 2004;165:35–52.
29. Braun RD, Lanzen JL, Snyder SA, Dewhirst MW. Comparison of tumor and normal tissue oxygen tension measurements using OxyLite or microelectrodes in rodents. *Am J Physiol Heart Circ Physiol* 2001;280:H2533–44.
30. Swartz HM, Khan N, Buckley J, et al. Clinical applications of EPR: overview and perspectives. *NMR Biomed* 2004;17:335–51.
31. Lord EM, Harwell L, Koch CJ. Detection of hypoxic cells by monoclonal antibody recognizing 2-nitroimidazole adducts. *Cancer Res* 1993;53:5721–6.
32. Gross MW, Karbach U, Groebe K, Franko AJ, Mueller-Klieser W. Calibration of misonidazole labeling by simultaneous measurement of oxygen tension and labeling density in multicellular spheroids. *Int J Cancer* 1995;61:567–73.
33. Emmenegger U, Morton GC, Francia G, et al. Low-dose metronomic daily cyclophosphamide and weekly tirapazamine: a well-tolerated combination regimen with enhanced efficacy that exploits tumor hypoxia. *Cancer Res* 2006;66:1664–74.
34. Ansiaux R, Baudelet C, Jordan BF, et al. Mechanism of reoxygenation after antiangiogenic therapy using SU5416 and its importance for guiding combined antitumor therapy. *Cancer Res* 2006;66:9698–704.
35. Airley R, Loncaster J, Davidson S, et al. Glucose transporter Glut-1 expression correlates with tumor hypoxia and predicts metastasis-free survival in advanced carcinoma of the cervix. *Clin Cancer Res* 2001;7:928–34.
36. Batchelor TT, Sorensen AG, di Tomaso E, et al. AZD2171, a pan-VEGF receptor tyrosine kinase inhibitor, normalizes tumor vasculature and alleviates edema in glioblastoma patients. *Cancer Cell* 2007;11:83–95.
37. Hlatky L, Hahnfeldt P, Folkman J. Clinical application of antiangiogenic therapy: microvessel density, what it does and doesn't tell us. *J Natl Cancer Inst* 2002;94:883–93.
38. Tuettenberg J, Friedel C, Vajkoczy P. Angiogenesis in malignant glioma—a target for antitumor therapy? *Crit Rev Oncol Hematol* 2006;59:181–93.
39. Rini BI. Vascular endothelial growth factor-targeted therapy in renal cell carcinoma: current status and future directions. *Clin Cancer Res* 2007;13:1098–106.
40. Jubb AM, Oates AJ, Holden S, Koeppen H. Predicting benefit from anti-angiogenic agents in malignancy. *Nat Rev Cancer* 2006;6:626–35.
41. Beecken WD, Fernandez A, Jousseaume AM, et al. Effect of antiangiogenic therapy on slowly growing, poorly vascularized tumors in mice. *J Natl Cancer Inst* 2001;93:382–7.
42. Fenton BM, Paoni SF, Grimwood BG, Ding I. Disparate effects of endostatin on tumor vascular perfusion and hypoxia in two murine mammary carcinomas. *Int J Radiat Oncol Biol Phys* 2003;57:1038–46.
43. Fenton BM, Paoni SF, Ding I. Effect of VEGF receptor-2 antibody on vascular function and oxygenation in spontaneous and transplanted tumors. *Radiother Oncol* 2004;72:221–30.
44. Segers J, Fazio VD, Ansiaux R, et al. Potentiation of cyclophosphamide chemotherapy using the anti-angiogenic drug thalidomide: importance of optimal scheduling to exploit the 'normalization' window of the tumor vasculature. *Cancer Lett* 2006;244:129–35.
45. Nakahara T, Norberg SM, Shalinsky DR, Hu-Lowe DD, McDonald DM. Effect of inhibition of vascular endothelial growth factor signaling on distribution of extravasated antibodies in tumors. *Cancer Res* 2006;66:1434–45.
46. Fenton BM, Paoni SF. The addition of AG-013736 to fractionated radiation improves tumor response without functionally normalizing the tumor vasculature. *Cancer Res* 2007;67:9921–8.
47. Huber PE, Bischof M, Jenne J, et al. Trimodal cancer treatment: beneficial effects of combined antiangiogenesis, radiation, and chemotherapy. *Cancer Res* 2005;65:3643–55.
48. Bertolini F, Paul S, Mancuso P, et al. Maximum tolerable dose and low-dose metronomic chemotherapy have opposite effects on the mobilization and viability of circulating endothelial progenitor cells. *Cancer Res* 2003;63:4342–6.